Evaluation of metal cation effects on galvanic corrosion behavior of the A5052 aluminum alloy in low chloride ion containing solutions by electrochemical noise impedance

M. Sakairi[1)], R. Sasaki[2)], A. Kaneko[3)], Y. Seki[3)], D. Nagasawa[3)]

[1)]Faculty of Engineering, Hokkaido University, Sapporo, Japan

[2)]Graduate School of Engineering, Hokkaido University

[3)] Nikkei Research & Development Center, Nippon Light Metal Co. Ltd., Shizuoka, Japan

Key word: Metal cation, aluminum alloy, galvanic corrosion, electrochemical noise impedance, FFT

Abstract

The effects of metal cations on the galvanic corrosion behavior of the A5052 aluminum alloy in low chloride ion containing solutions (tap water) were examined by electrochemical noise impedance. The electrochemical noise impedance and conductance were calculated by the power spectral density (PSD) of the galvanic current and potential. The oscillations in the galvanic current correlate well with the oscillations in the potential. The total charge (summation of galvanic current) during galvanic corrosion tests was suppressed by the addition of Ca^{2+}, while it was increased with Mg^{2+} addition. Only a small effect on mean impedance and conductance was observed in solutions with Cu^{2+} and Mg^{2+}, while addition of Ca^{2+} strongly influences both the mean impedance and conductance. These results may be explained by the passive film structure changes due to the metal cations. The results obtained in this study indicate that metal cations play a very important role in the corrosion behavior of A5052 aluminum alloys in tap water.

1. Introduction

Aluminum alloys show high corrosion resistance in a wide range of environments and together with their high strength/weight ratios. These properties have been made aluminum alloys widely used. The high corrosion resistance is due to protective oxide films, passive films, formed on the alloys. Generally, the corrosion rate of aluminum alloys depends on the concentration of chloride ions and the pH of the particular environments, and it is considered that only little corrosion of aluminum alloys occurs in very dilute chloride solutions such as tap waters and fresh water. There are only few studies focused on the corrosion of aluminum and aluminum alloys in tap water [1-9].

Some of the authors here have also investigated the effect of metal cations on the corrosion behavior of aluminum alloys in model tap waters [10-16], and found that the corrosion behavior of A3003 strongly depends on the kinds of metal cations in the environments. The effect of metal cations has been explained by using the metal cation hardness concept which is based on a hard and soft acid and base, HSAB, concept [17, 18]. According to the HSAB concept, the hard metal cations in a solution attract the electron pair of oxygen atoms in H_2O or OH in the passive film. Therefore, as hard metal cations in the solutions adsorb on the oxygen atoms of H_2O or OH in the passive film, they may be more easily replaced with the proton of H_2O in the passive film (when compared with softer metal cations). From a surface analysis by Auger electron spectroscopy (AES) and X-ray photoelectron spectroscopy (XPS) after immersion corrosion tests, the harder metal cations were found to be incorporated in the oxide films [14-16].

The aluminum alloys are widely used in heat exchangers especially in automotive applications. There are many reports focused on the corrosion of the alloys used here [19-21]. Because of limitations on copper resources, aluminum alloys are used in air conditioners and home heating systems. When using aluminum alloys in home heating systems, which used tap water, galvanic corrosion must be taken into account. There are many reports of galvanic corrosion of aluminum in high concentration solutions such as 5 mass% NaCl solutions [22-24]. Murer et al. reported numerical modeling of the galvanic coupling of aluminum and aluminum alloys, and used results of a scanning vibrating electrode technique to propose a model to explain the results [25]. However, no reports have focused on effect of metal cations on galvanic corrosion of aluminum alloys in low

chloride ion containing solutions (fresh or tap waters). In this study, electrochemical noise analysis and impedance techniques are applied to evaluate the effect of metal cations on galvanic corrosion of an aluminum alloy in low chloride ion containing solutions.

2. Experimental

2.1 Specimens

Aluminum sheets (20 × 30 mm, thickness 1.2 mm) of A5052 aluminum alloy were used as specimens and Table 1 shows the chemical composition. Before the tests, specimens were chemically etched in 0.1 kmol m^{-3} NaOH solutions and then cleaned in ethanol and in doubly distilled water in an ultrasonic bath. After cleaning, the specimens were sealed by silicone resin, to ensure that a 15 mm × 15 mm area on one side would be in contact with the solutions.

2.2 Solutions

The low chloride ion containing solution used was 0.5 kmol m^{-3} H_3BO_3 - 0.05 kmol m^{-3} $Na_2B_4O_7$ (borate, pH = 7.4) with four different salts mixed into the solution (Table 2), as following: 1 mol m^{-3} NaCl (Na), 0.3 mol m^{-3} $CaCl_2$ + 0. 4 mol m^{-3} NaCl (Ca + Na), 0.3 mol m^{-3} $MgCl_2$ + 0.4 mol m^{-3} NaCl (Mg + Na), and 0.3 mol m^{-3} $CuCl_2$ + 0.4 mol m^{-3} NaCl (Cu + Na). The corrosion behavior of aluminum alloys strongly depends on the pH of solutions, and the pH of tap water is closed to neutral. The total ion concentration of borate in the solutions here is higher than that in usual tap waters, however, to avoid a pH effect on the corrosion behavior, borate was selected as the basic solution in this study. The chloride ion also plays an important role in corrosion, therefore, the concentration of chloride ions in all of the solutions was set to 1 mol m^{-3}, similar to that of usual tap water. The total ion concentration of the solutions is higher than that of usual tap water, however, with the similar pH and chloride ion concentration, the solutions used in this study can be considered similar to usual tap water. All chemicals were commercially available special grade and obtained from Kanto Chemical Co. Ltd. The main metal cation contained in the solutions is Na^+, and by addition of the different salts it is possible to investigate the effect of the minor and/or added metal cations. The calculated metal cation hardness [17, 18] is reported as follows, Na^+; 1.01, Ca^{2+}; 2.75, Mg^{2+}; 3.54, and Cu^{2+}; 5.14. The NaCl added

solution was used as the reference solution for the corrosion behavior of the other metal cation containing solutions.

2.3 Galvanic corrosion test and surface ovservation

Specimens were dipped in still (un-agitated) solutions at room temperature, and then connected to a Pt plate with 18 cm^2 to form a galvanic couple (Fig. 1). To avoid changes in the cathodic reaction, a relatively large area size Pt plate was used as the cathode. The main cathodic reaction in this study is oxygen reduction. The galvanic current, aluminum dissolution, showed a plus current, and the specimen potentials during the tests were measured for 86.4 ks (24 h). An electrometer (R8240, ADVANTEST co.) is used for measurement of galvanic current, and multi-meter (R6452A ADVANTEST co.) is used for measurement of specimen potential. The data acquisition interval in the computer is 3 s and an Ag/AgCl sat. KCl electrode was used as reference electrode. The records of the current and the potential were processed by calculating the Power Spectral Density (PSD) by the Fast Fourier Transform (FFT) method with 1024 data points (3072 s), and the electrochemical noise impedance was calculated by using this current and potential PSD. Both the current and the potential PSD, and the electrochemical noise impedance calculations were carried out from each data point from 0 s to 80 ks.

After the galvanic corrosion tests, specimen surfaces were examined by a confocal scanning laser microscope (CSLM; 1SA21, LASERTEC Co.).

3. Results and discussion

3.1 Galvanic corrosion results

Figure 2 shows changes in potential and current density during the galvanic corrosion tests for the total length of experiments (top tow) and expanded for the period from 20 ks to 25 ks (bottom tow), in borate with a) and c) 1.0 mol m^{-3} NaCl, and b) and d) 0.3 mol m^{-3} $CaCl_2$ + 0. 4 $molm^{-3}$ NaCl. In both solutions, the potential suddenly decreases after connecting the specimen to the Pt electrode and then decreases with immersion time, while the mean value of the current density shows a smaller change. Both the potential and the current density clearly show fluctuations, and the current density fluctuations and potential fluctuations

shows good correlation (Fig. 2 b) and d)), such as the potential decreases the current increases, and potential increases current decreases.

Figure 3 shows CSLM images after the galvanic corrosion tests in the four solutions. There are corrosion pits in all solutions suggesting that the fluctuations in Fig. 2 may be attributed to pitting corrosion events. Each fluctuation shows the start, propagation, and discontinuation of the pitting process.

The total charge density (summation of the current density from 0 to 86.4 ks) with the different metal cation containing solutions is shown in Fig. 4. The total charge density of the Cu^{2+} and Ca^{2+} added solutions is lower than with the Na^{+} solution, while it is higher with the Mg^{2+} addition. This result indicates that the galvanic corrosion rate is affected by the kind of metal cations in the test solutions.

3.2 Electrochemical noise impedance

Figure 5 shows an example of the potential PSD and current density PSD, and the electrochemical noise impedance calculated using the galvanic corrosion data in Fig. 2 a) as a function of frequency, f. Both the potential PSD and the current density PSD show one flat area at $f = 2 \times 10^{-3}$ - 2×10^{-2} s^{-1}. The slope of the potential at the high frequency range, $f > 2 \times 10^{-2}$ s^{-1} is about -1 and with the current density PSD it is about 0.6. The electrochemical noise impedance shows no frequency dependence at $f < 2 \times 10^{-2}$ s^{-1}, while there appears to be a frequency dependence at $f > 2 \times 10^{-2}$ s^{-1} with a slope of about -0.5.

The average values at flat area (around $f = 5 \times 10^{-3}$ s^{-1}) of the potential PSD, the current density PSD, and the electrochemical noise impedance were calculated, and then plotted as galvanic test time. One example of these values calculated using Fig. 2 a) is shown in Fig. 6. The averages of PSD in both potential and current density show fluctuations of a similar appearance and the tendencies correlate well. The average of the electrochemical noise impedance shows an almost unchanged value throughout the galvanic corrosion tests with spike type fluctuations, bottom in Fig. 6.

Average of flat area of electrochemical impedance PSD as a function of experimental time in a) Cu+Na, b) Mg+Na and c) Ca+Na solutions are showen in Fig. 7. The spike type fluctuations are observed in both solutions, and large fluctuations are also observed in

Cu+Na and Ca+Na. In the Mg+Na, the average of the impedance slowly decreases with time, meaning corrosion resistance decreases with time.

The electrochemical noise impedance is related to the corrosion resistance, and the conductance (inverse of the electrochemical noise impedance) is related to corrosion rate or corrosion inhibition ability by the passive film on the specimens. The mean values of the electrochemical noise impedance and conductance in the solutions were calculated, and the results are shown in Fig. 8. The mean impedance and conductance in the solutions with added Na^{+} and Mg^{2+} are very similar while the solution with Ca^{2+} shows a large influence on both the mean impedance and conductance. This impedance results and result shown in Fig. 4 indicates that the minor metal cation plays an important role in the galvanic corrosion behavior of A5052 aluminum alloys in tap water. The results shown in here also suggest that the effect of metal cations must be considered to evaluate the corrosion behavior of A5052 aluminum alloys in tap water.

3. 3 Role of metal cations on the corrosion behavior

From the HSAB concept, harder metal cations have a stronger affinity to OH^{-} [17]. Hard metal cations in solution attracts the electron pair of the oxygen atom in H_2O or OH in the passive film and that pair can then be more easily replaced with the proton of the H_2O molecule in a passive film [18]. This may reduce the number of flaws in the passive film or it may increase the re-passivation rate. Fig. 9 shows a schematic outline of the de-protonation process by Ca^{2+}. From XPS and Auger analysis, there is no evidence of Ca^{2+} incorporation in the passive film [14 - 16], however, this is one possible reason why only very small amounts of Ca^{2+} increases the corrosion resistance of A5052 aluminum alloy in the solutions.

The metal cation hardness of Cu^{2+} is higher than that of Ca^{2+}, however, no significant change of galvanic corrosion behavior was observed with the Cu^{2+} added solutions. The redox potential of Cu^{2+} - Cu is 0.337 V vs. SHE [26], this indicates that copper would easily be deposited on the electrode, and copper deposition was observed on the Pt electrode after the galvanic corrosion tests. The deposition reduces the concentration of Cu^{2+} in the solution to reduce the amount of de-protonation by Cu^{2+}, therefore, Cu^{2+}

addition had little influence on the galvanic corrosion behavior of the A5052 aluminum alloys in this study.

The metal cation hardness of Mg^{2+} is also higher than that of Ca^{2+}, and it may be expected that the addition of Mg^{2+} should reduce the corrosion rate of the alloy. With Ca^{2+}, however, there was an increase in the galvanic corrosion rate of the A5052 aluminum alloy with Mg^{2+} addition of the solutions. The Pilling-Bedworth ratio [27] of MgO is 0.81, meaning that MgO cannot fully cover the substrate surface. Therefore, incorporation of Mg^{2+} into the passive film may induce shrinkage of the film, in turn inducing flaws, and reducing its corrosion protection ability of the film. Therefore, galvanic corrosion resistance in the Mg^{2+} containing solutions did not increase.

To further clarify the inverse effect of Mg^{2+} and Cu^{2+} on the galvanic corrosion behavior expected from metal cation hardness theory, further investigation is required. Moreover, a more sophisticated model is required to explain the role of metal cations on the corrosion behavior of aluminum alloys in usual tap water.

4. Conclusions

The effects of metal caions on the galvanic corrosion behavior of A5052 aluminum alloy in low chloride ion containing solutions (tap water) were examined by electrochemical noise impedance. Both current and potential fluctuations are measured during the galvanic corrosion tests, and these considered to be related to pitting events. These are also showed good correlation.

The electrochemical noise impedance and the total charge (summation of galvanic current during galvanic corrosion tests) are affected by the added metal cations. Additions of Ca^{2+} and Cu^{2+} decrease total charge, and Ca^{2+} increases the galvanic corrosion resistance, while Mg^{2+} shows not significantly change on the galvanic corrosion resistance. The effect of Mg^{2+} on the galvanic corrosion behavior may be explained by low value of Pilling-Bedworth ratio of its oxide.

References

[1] H.J, Goug, D. G. Sopwith, Proceedings of the Royal Society of London, Series A: Mathematical, Physical and Engineering Sciences 135 (1932) 392.

[2] Y. Baba, M. Hagiwara, Sumitomo Keikinzoku Giho 9 (1968) 208.
[3] N. Gugliemi, International Leichtmetalltag 5 (1969) 39.
[4] I. Uchiyama, K. Ohno, E. Sato, Aruminyumu Kenkyu Kaishi 103 (1976) 67.
[5] N. Kanani, Aluminum 55 (1979) 724.
[6] M. C. Reboul, Corrosion 35 (1979) 423.
[7] T. Sakaida, H. Ikeda, Z. Tanabe, Sumitomo Keikinzoku Giho 26 (1985) 221.
[8] K. Furumata, T. Suzuki, J. Kobayashi, O. Seri, Keikinzoku 51 (2001) 242.
[9] K. Otani, M. Sakairi, T. Kikuchi, A. Kaneko, Zairyo-to-Kankyo 59 (2010) 330.
[10] M. Sakairi, Y. Shimoyama, D. Nagasawa, Corrosion Science and Technology 7 (2008) 168.
[11] M. Sakairi, A. Kaneko, Y. Seki, D. Nagasawa, Proceedings of Eurocorro2008 (2008) 2185.
[12] M. Sakairi, A. Kaneko, T. Kikuchi, Y. Seki, D. Nagasawa, Proceedings of Eurocorr2009 (2009) NO. SS 17-0-7947.
[13] M. Sakairi, A. Kaneko, K. Otani, Y. Seki, D. Nagasawa, Proceedings of 18th International Corrosion Congress10 (2011) 533 (10 pages).
[14] M. Sakairi, Y. Otani, A. Kaneko, Y. Seki, D. Nagasawa, Surface and Interface Analysis, 45 (2013) 1517.
[15] M. Sakairi, K. Otani, A. Kaneko, Y. Seki, D. Nagasawa, Rust prevention and control Japan, 57, (2013) 147.
[16] M. Sakairi, K. Otani, R, Sasaki, A. Kaneko, Y. Seki and D. Nagasawa, Proceedings of Eurocorr2013, No. 1082 (2013).
[17] M. Misono, E. Ochiai, Y. Saito, Y. Yoneda, Journal of Inorganic and Nuclear Chemistry 29 (1967) 2685.
[18] S. Zhang, T. Shibata, T. Haruna, Corrosion Science 47 (2005) 1049.
[19] M. Edo, S. Kuroda, A. Watanabe, K. Tohma, Journal of Japan Institute of Light Metals, 52 (2003) 55.
[20] Y. Oya, Y. Kojima, Journal of the Japan Institute of Light Metals, 62 (2012) 244.
[21] Y. Oya, Y. Kojima, N. Hara, Materials Transactions, 54 (2013) 1200.
[22] A.B.M. Mujibur Raham, S. Kumar, A. R. Gerson, Corrosion Science, 49 (2007) 4339.

[23] J. Idrac, G. Mankowski, G. Thompson, P. Skeldon, Y. Kihn, C. Blanc, Electrochimica Acta, 52 (2007) 7626.
[24] K. B. Deshpande, Corrosion Science, 52 (2010) 281.
[25] N. Murer, R. Oltra, B. Vuillemin, O. Neel, Corrosion Science, 52 (2010) 130.
[26] M. Pourbaix, Atlas of electrochemical equilibria in aqueous solutions, Section 14.1, National Association of Corrosion Engineers, Huston, Texas (1974).
[27] N.B. Pilling, R. E. Bedworth, Journal of the Institute of metals, 29 (1923) 529.

Captions

Table 1 Chemical composition of A5005 aluminum alloy (mass%).

Table 2 List of used low chloride ion containing solutions.

Fig. 1 Schematic outline of the galvanic corrosion test equipment and experimental setup.

Fig. 2 Changes in potential and current density during galvanic corrosion test in borate with a) and c) 1.0 mol m^{-3} NaCl, and b) and d) 0.3 mol m^{-3} $CaCl_2$ + 0. 4 mol m^{-3} NaCl.

Fig. 3 CSLM images of specimen surfaces after galvanic corrosion tests in the four solutions.

Fig. 4 Total charge density (summation of current density from 0 to 86.4 ks) as a function of containing metal cations.

Fig. 5 Example of the potential power spectral density, PSD, (top panel), the current density power spectral density, PSD, (mid panel), and electrochemical noise impedance (bottom panel). These were calculated using the galvanic corrosion test results in Fig. 2 a).

Fig. 6 Average of flat area in Fig. 5 (at around $f = 5 \times 10^{-3}$ s^{-1}) of power spectral density, PSD, of the potential and current density, and the electrochemical impedance calculated using the galvanic corrosion test results in Fig. 2 a).

Fig. 7 Average of flat area of electrochemical impedance power spectral density, PSD, as a function of experimental time in a) Cu+Na, b) Mg+Na and c) Ca+Na solutions.

Fig. 8 Mean electrochemical noise impedance and conductance in the four solutions.

Fig. 9 Schematic outline of the deprotonation process by Ca^{2+}.

Table 1

Cu	Si	Fe	Mn	Mg	Zn	Cr	Ti	V	Zr	Al
<0.01	0.08	0.26	<0.01	2.61	0.01	0.17	0.02	0.01	<0.01	bal.

Table 2

Na	1 mol m^{-3} NaCl+0.5 kmol m^{-3} H_3BO_3 - 0.05 kmol m^{-3} $Na_2B_4O_7$
Ca+Na	[0.3 mol m^{-3} $CaCl_2$ + 0. 4 mol m^{-3} NaC] +0.5 kmol m^{-3} H_3BO_3 - 0.05 kmol m^{-3} $Na_2B_4O_7$
Mg+Na	[0.3 mol m^{-3} $MgCl_2$ + 0.4 mol m^{-3} NaCl]+0.5 kmol m^{-3} H_3BO_3 - 0.05 kmol m^{-3} $Na_2B_4O_7$
Cu+Na	[0.3 mol m^{-3} $CuCl_2$. + 0.4 mol m^{-3} NaCl]+0.5 kmol m^{-3} H_3BO_3 - 0.05 kmol m^{-3} $Na_2B_4O_7$

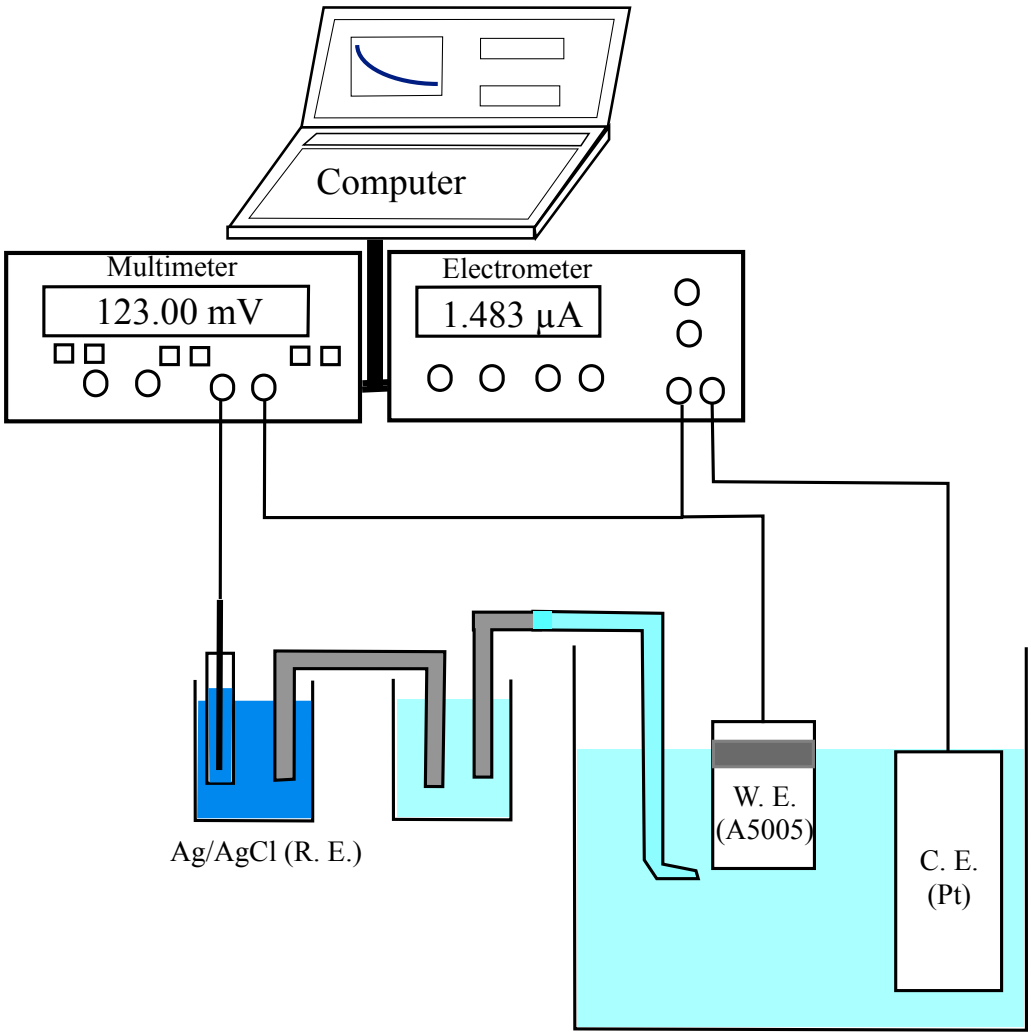
Computer
Multimeter
123.00 mV
Electrometer
1.483 µA
Ag/AgCl (R. E.)
W. E.
(A5005)
C. E.
(Pt)

Fig. 1

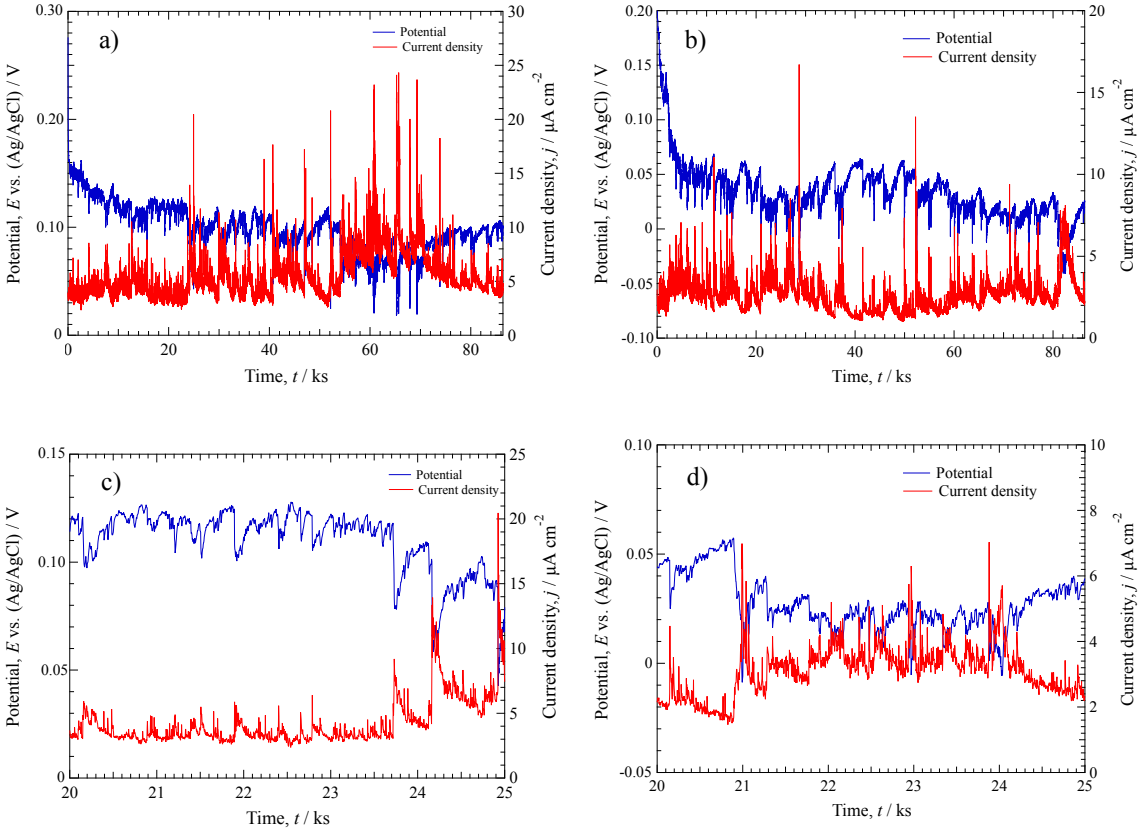
a)
b)
c)
d)
Potential
Current density
Potential, E vs. (Ag/AgCl) / V
Current density, j / μA cm-2
Time, t / ks

Fig. 2

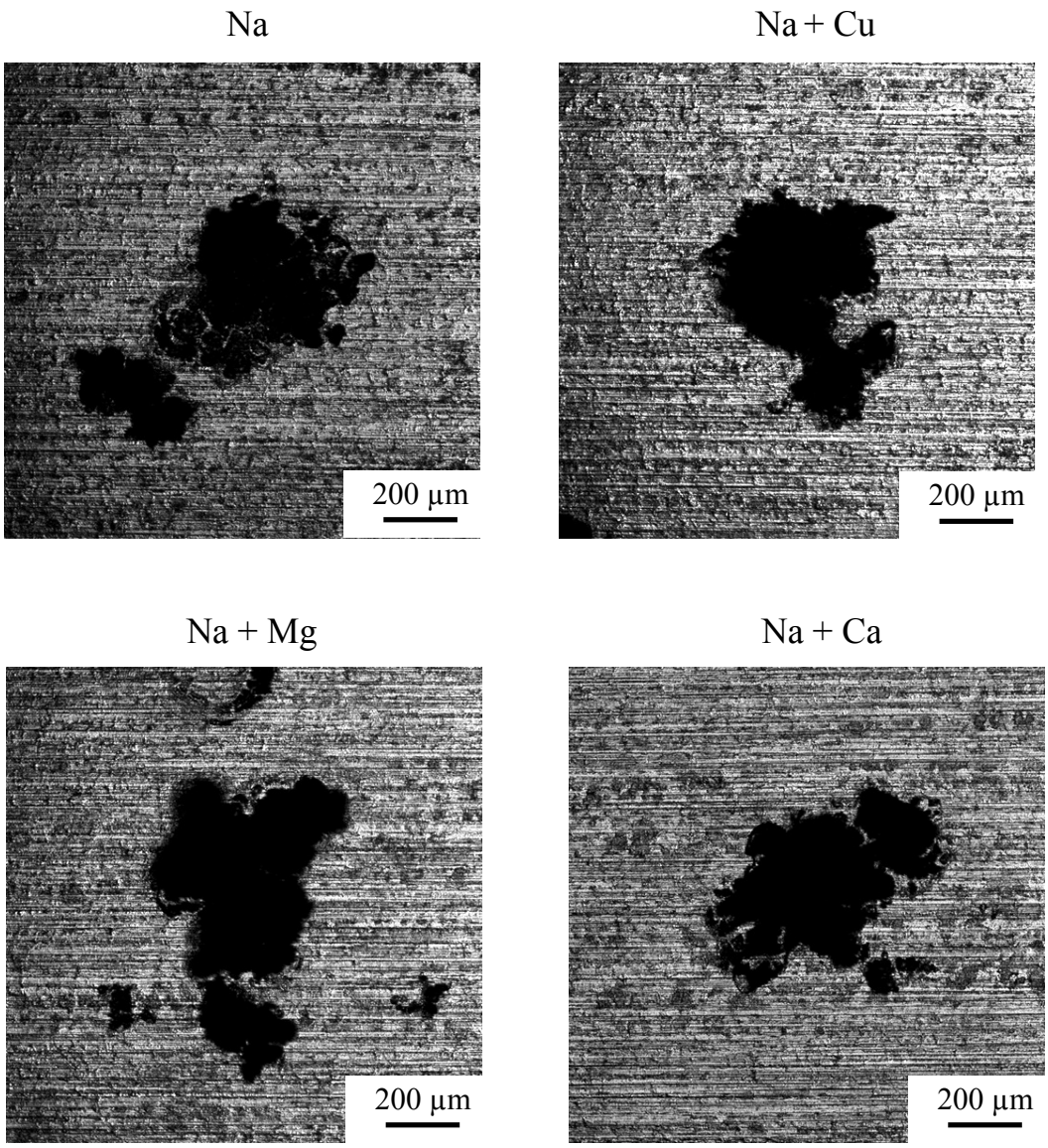

Fig. 3

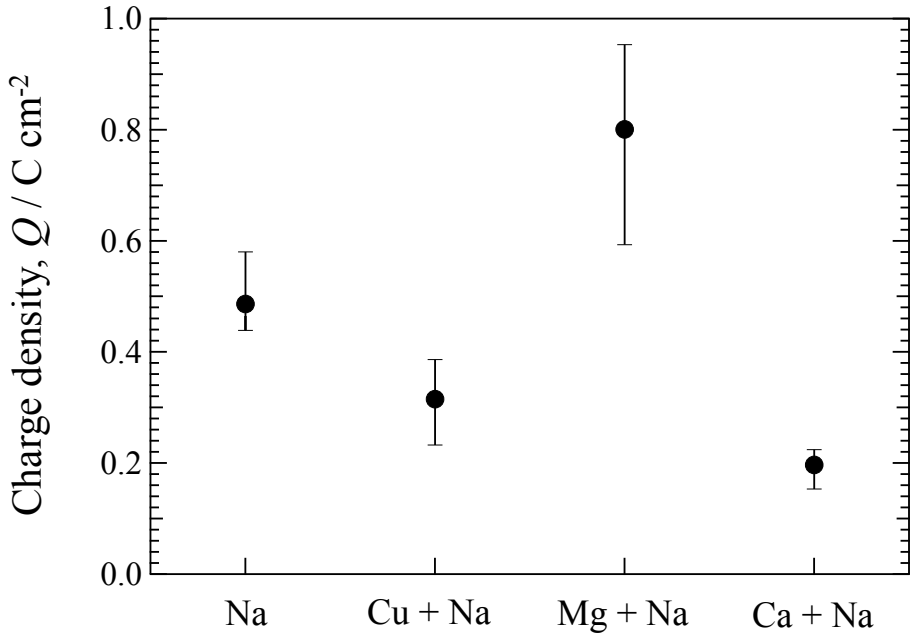

Fig. 4

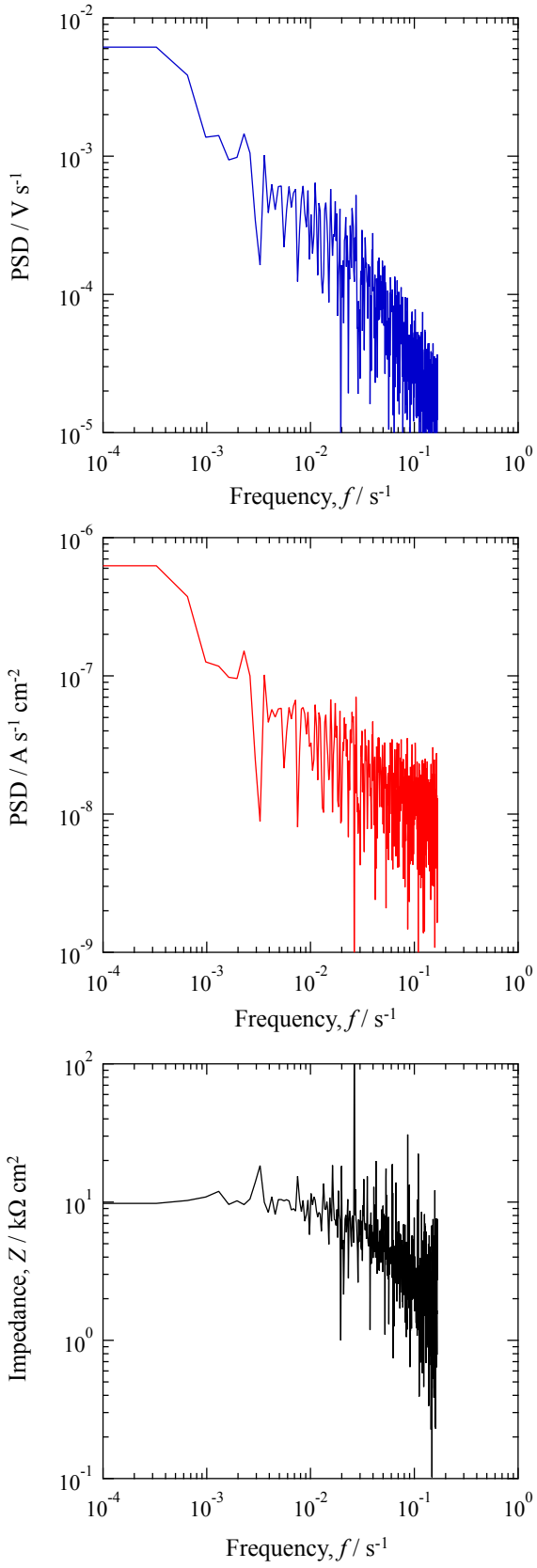
PSD / V s-1
Frequency, f / s-1
PSD / A s-1 cm-2
Frequency, f / s-1
Impedance, Z / kΩ cm2
Frequency, f / s-1

Fig. 5

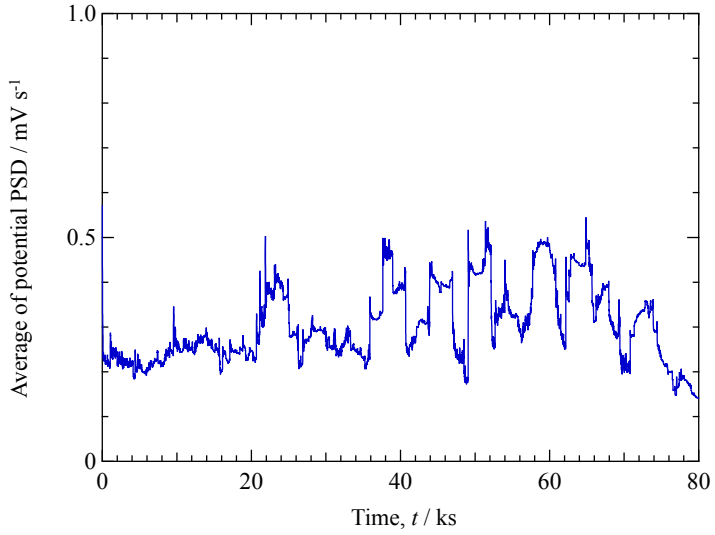
1.0
0.5
0
Average of potential PSD / mV s-1
0
20
40
60
80
Time, t / ks

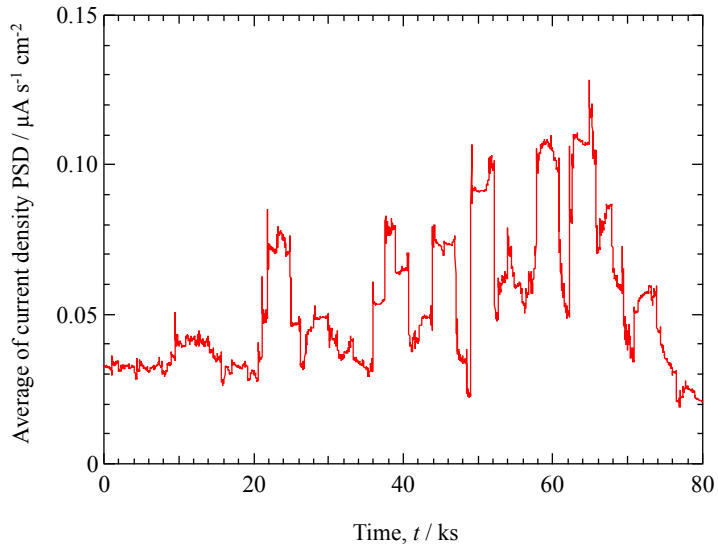
0.15
0.10
0.05
0
Average of current density PSD / μA s-1 cm-2
0
20
40
60
80
Time, t / ks

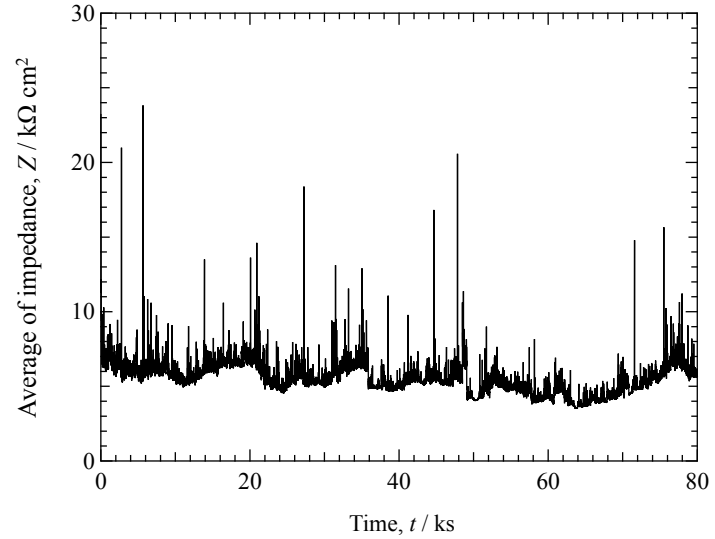
30
20
10
0
Average of impedance, Z / kΩ cm2
0
20
40
60
80
Time, t / ks

Fig. 6

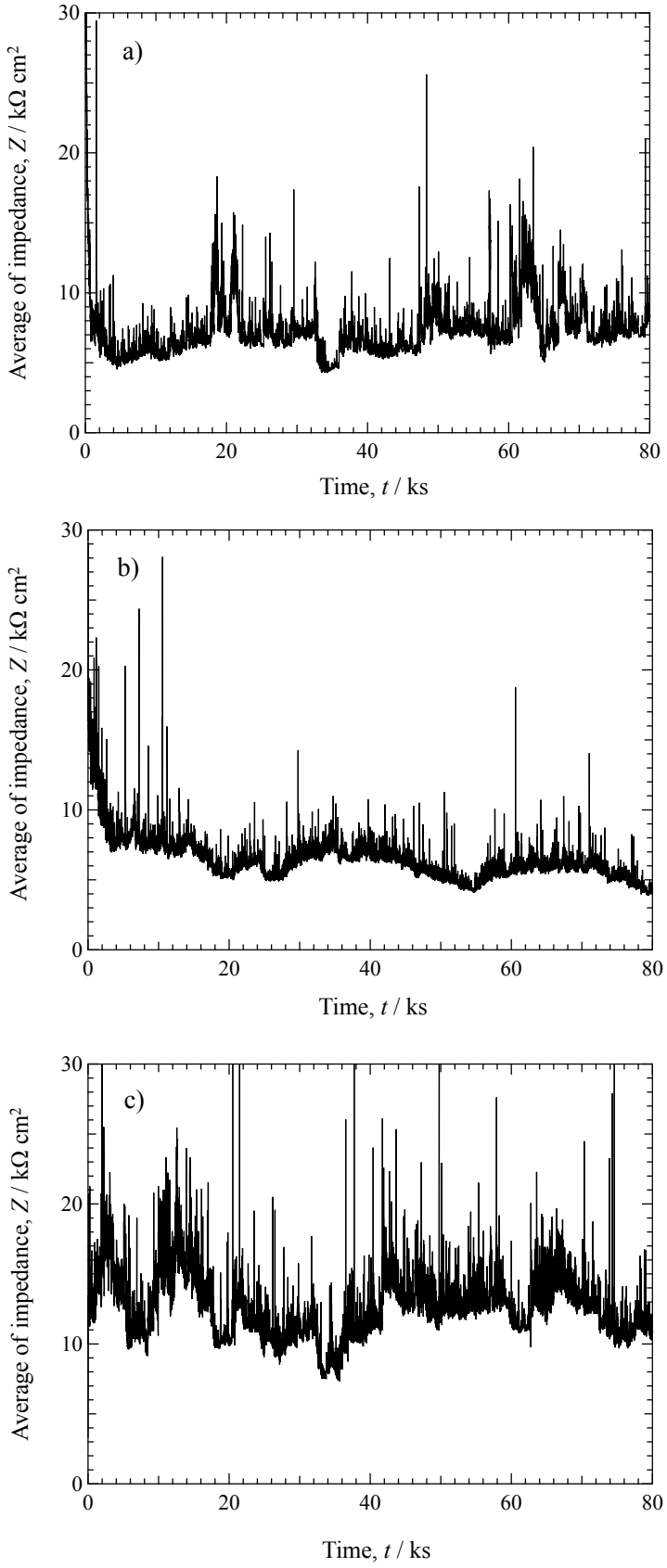
a)
b)
c)
Average of impedance, Z / kΩ cm²
Time, t / ks
0
10
20
30
0
20
40
60
80

Fig. 7

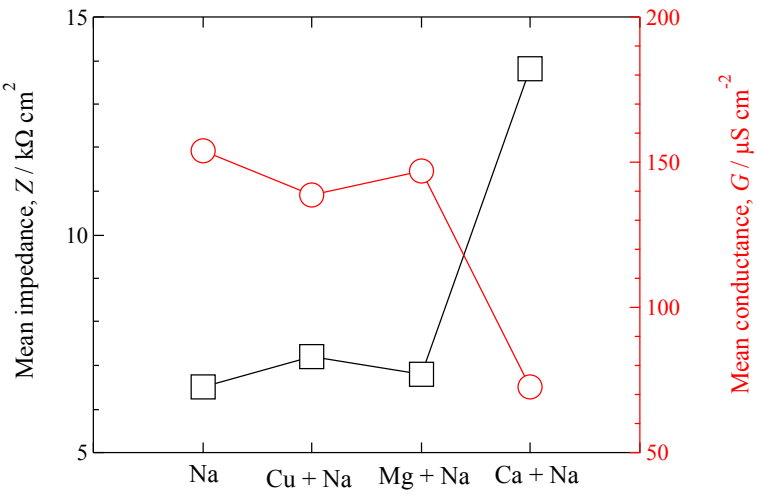
15
10
5
200
150
100
50
Mean impedance, Z / kΩ cm2
Mean conductance, G / µS cm-2
Na
Cu + Na
Mg + Na
Ca + Na

Fig. 8

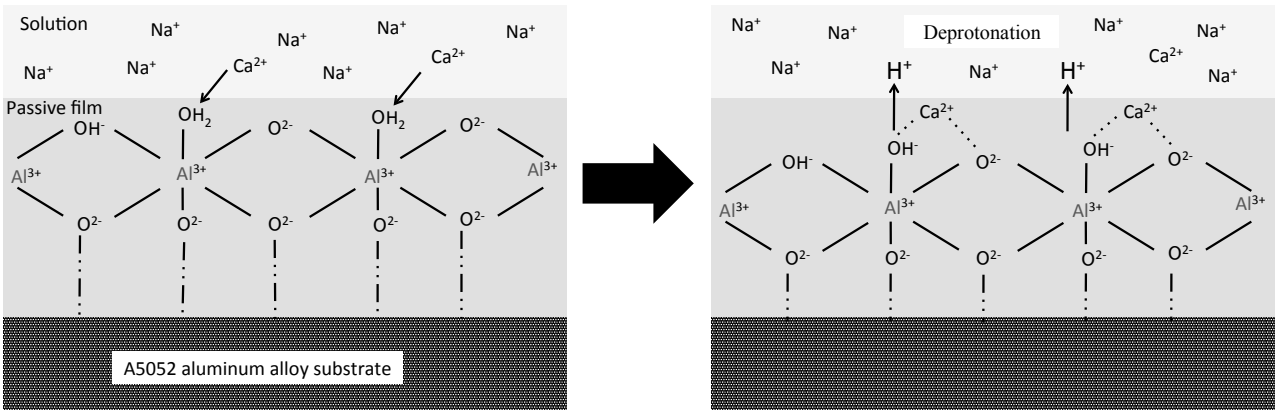

Passive film structure changes with addition of Ca^{2+}

Fig. 9